Deadline-aware Task Scheduling for Solar-powered Nonvolatile Sensor Nodes with Global Energy Migration *

Daming Zhang[1], Yongpan Liu[1], Xiao Sheng[1], Jinyang Li[1], Tongda Wu[1], Chun Jason Xue[2], Huazhong Yang[1]
[1]Tsinghua National Laboratory for Information Science and Technology (TNList)
[1]Department of Electronic Engineering, Tsinghua University, Beijing, China, 100084
[2]Department of Computer Science, City University of Hong Kong, Hong Kong, China, 999077
ypliu@tsinghua.edu.cn, zdm06@mails.tsinghua.edu.cn

ABSTRACT

Solar-powered sensor nodes with energy storages are widely used today and promising in the coming trillion sensor era, as they do not require manual battery charging or replacement. The changeable and limited solar power supply seriously affects the deadline miss rates (DMRs) of tasks on these nodes and therefore energy-driven task scheduling is necessary. However, current algorithms focus on the single period (or the current task queue) for high energy utilization and suffer from bad long term DMR. To get better long term DMR, we propose a long term deadline-aware scheduling algorithm with energy migration strategies for distributed super capacitors. Experimental results show that the proposed algorithm reduces the DMR by 27.8% and brings less than 3% of the total energy consumption.

Keywords

Energy Harvesting and Migration, Long Term Deadline-aware Scheduling, Nonvolatile Sensor Node, Capacitor Sizing

1. INTRODUCTION

Due to the requirements for mobility and portability, most of wireless sensor nodes are powered by batteries and need frequent maintenance. However, as the era of trillion sensors is coming, the rapid increasing number of sensor nodes makes the maintenance prohibitively expensive. Self-powered sensor nodes, which provide potentially maintenance-free features, are attracting more and more interests. There are various energy harvesting technologies, such as solar, thermal, wireless and vibration energy harvesting. Among them, solar energy is one of the most promising ones, thanks to the high power density, the high efficiency and the wide range of the output voltage and current. In fact, solar-powered sensor nodes are widely studied for wearable devices, environmental and structural monitoring, etc.

Those applications require sensor nodes to collect data day and night, where periodic sensing and processing need to be done before their deadlines. It is a big challenge for solar-powered sensor nodes to guarantee good quality of service (QoS) due to the power variance. Thus, the mismatch between power supply and consumption happens. When there is no enough energy, the node shuts down and the tasks may miss their deadlines. It will lead to bad QoS. Though it is possible to use over-designed solar cells, it will lead to a significant increasing in cost and volume. As wireless sensor nodes, such as wearable devices, are quite sensitive to volume and price, the over-design approach is unacceptable in practice. To handle such a problem, energy-driven task scheduling is one of the promising techniques to make solar-powered sensor nodes small, cheap and reliable.

Lots of task scheduling algorithms for solar-powered sensor nodes have been presented. According to the strategies used to match power supply and consumption, they can be classified into four categories. First approaches [1, 2, 3] adopted lazy scheduling algorithms (LSAs) to determine the start time of each task, which can get the maximum energy utilization with the given solar power. Furthermore, task decomposition and combination were proposed [4] to realize more accurate and flexible load matching. Third, dynamic voltage and frequency scaling (DVFS) was integrated in load matching algorithms [5, 6] for better DMR. Researchers further improved this approach by considering super capacitor charging efficiency [7] and multi-core systems [8]. Most recently, an intra-task scheduling method with fine-grained load matching [9] was proposed. It performed quite well on the storage-less and converter-less solar-powered sensor nodes [10].

However, all previous scheduling algorithms focus on matching power supply and consumption in a single period, whose objective is to achieve the best DMR in the present period. Due to lacking a big map on the long term solar power, they tend to achieve a local optimal DMR solution instead of a global optimal one in a long term sense. Furthermore, with the long term solar power in mind, energy migration should be adopted for better DMR. As the energy migration efficiency is related to the capacitor size, migration quantity and distance, an optimal capacitor sizing and selection solution should be developed.

Therefore, we proposed a deadline-aware task scheduling algorithm for better long term (up to several days) DMR, which is targeted on a dual-channel solar-powered sensor node [11] with distributed capacitors. Our specific contributions are listed as below:

- We propose a dual-channel solar-powered sensor node architecture, which consists of a high efficient direct supply channel and a "store and use" channel with distributed capacitors, and the system model is extracted from the novel structure.
- We develop a diagram to optimize long term DMR with efficient energy migration, which contains offline and online parts. The former determines the optimal capacitor sizes and DMR training samples for artificial neural network (ANN) training. The later adopts the ANN to determine the real-time optimal capacitor size, scheduling pattern and task queue, followed by an algorithm for better DMR.
- The proposed method achieves 27.8% better DMR compared with previous works for real benchmarks. The efficiency of energy migration can be boosted up to 30.5% if multiple values of super capacitors are used based on the migration patterns.
- Counterintuitively, we find that the traditional highest energy

*This work was supported in part by High-Tech Research and Development (863) Program under contract 2013AA01320 and Huawei Shannon Lab and the Importation and Development of High-Caliber Talents Project of Beijing Municipal Institutions under contract YETP0102.

DAC '15, June 07 - 11, 2015, San Francisco, CA, USA

http://dx.doi.org/10.1145/2744769.2744815.

utilization algorithm does not necessarily guarantee better DMR and there exists a balance point on the prediction length for long term DMR optimization due to the locality of correlation in solar power.

2. OVERVIEW

This section first shows the motivation for long term deadline-aware scheduling and capacitor sizing. After that, the architecture of the sensor node and the diagram of the proposed algorithm are presented.

2.1 Motivating examples

Figure 1 shows why long term deadline-aware scheduling is superior than the traditional one. Since the traditional method pursues the local optimal DMR in the present period, it may be better during the day but suffers from very bad DMR at night. However, the proposed one achieves much better DMR at night and therefore better DMR in total. Therefore, we need a long term deadline-aware scheduling for better QoS all the time.

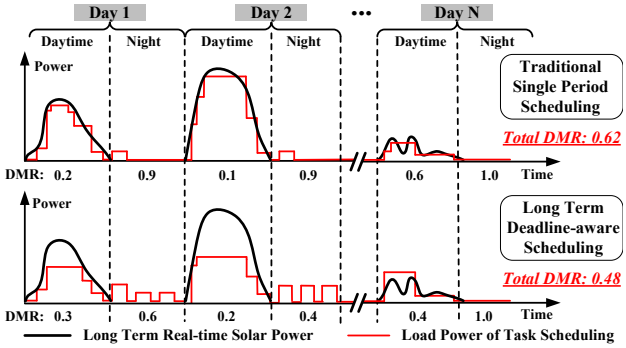

Figure 1: Motivation for long term deadline-aware scheduling

With long term DMR in mind, the positive energy migration should be done. Though it can be done with a single super capacitor, Figure 2 demonstrates that distributed super capacitors provide much higher migration efficiency. Intuitively, a small super capacitor is better to move a small quantity of energy in a short time, since the charging and discharging energy loss of the super capacitor in high voltages are smaller. In this case, the charging and discharging denote the efficiency. However, a large super capacitor will be better if a large quantity of energy is migrated for a long time, since a lower voltage of the super capacitor will lead to much smaller leakage. In this case, the leakage dominates due to the long migration time [12]. Therefore, an optimal size exists for a super capacitor under certain solar power and workload, which shows the necessity of super capacitor sizing.

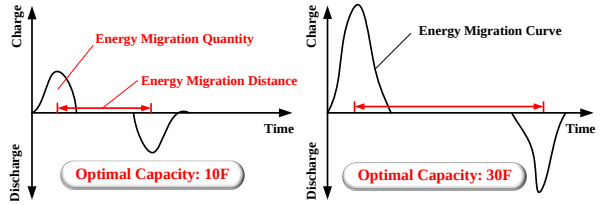

Figure 2: Motivation for distributed super capacitor sizing

Long term deadline-aware scheduling will bring prohibitive complexity for the optimization, since any task can be executed at any time during several days and multiple capacitors can be selected to power the sensor node. The complexity has an exponential relationship with the numbers of tasks, time slots and capacitors for scheduling. Therefore, an efficient solution is badly needed for such a complex optimizing problem..

2.2 Architecture and proposed algorithm

We target the algorithm on a high energy efficient architecture of solar-powered nonvolatile sensor node (see Figure 3). It contains a direct supply channel and a "store and use" channel using distributed super capacitors (SCs) for energy migration. Based on the scheduling results, the power management unit (PMU) switches the power supply channels, selects the super capacitors, and determines the multiple nonvolatile processors (NVPs) [13, 14] for task execution.

Figure 4 gives the diagram for long term deadline-aware scheduling, which contains offline and online parts. The offline part first executes the super capacitor sizing step. Long term DMR optimization is then performed to get the optimal samples, which are used for offline ANN training. The online part is a joint coarse / fine-grained deadline-aware scheduling algorithm. In this algorithm, the optimal super capacitor, the scheduling pattern and the tasks executed in a single period are calculated by the ANN-based long term deadline-aware analysis (coarse-grained). After that, the intra / inter-task scheduling algorithm, is executed in each time slot of the period (fine-grained).

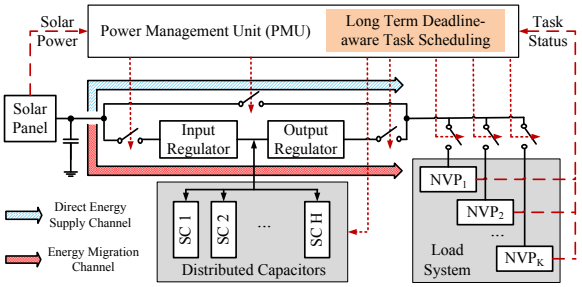

Figure 3: Architecture of dual-channel solar-powered sensor node

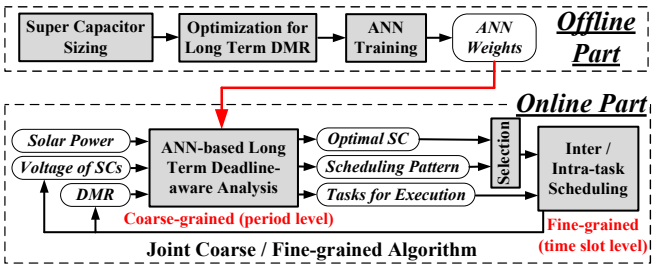

Figure 4: Diagram of long term deadline-aware task scheduling

3. SYSTEM MODELING

This section describes the system model of the proposed architecture and defines the variables for long term deadline-aware scheduling. The problem formulation is then presented.

Table 1: Parameters and variables of the system model

	Symbol	Description
Time	N_d	Number of days for task scheduling
	$(N_p, \Delta T)$	Number of periods in one day, each period lasting ΔT (s)
	$(N_s, \Delta t)$	Number of slots in one period, each slot lasting Δt (s)
Task	V	Task set, $V = \{\tau_1, \tau_2, \cdots, \tau_N\}$
	D_n	Deadline of τ_n in each period (s)
	S_n	Total execution time of τ_n in each period (s)
	P_n^τ	Average execution power of τ_n (mW)
	$W_{n,l}$	Task dependence from τ_n to τ_l
System	$P^s_{i,j,m}$	Average solar power of the mth time slot in the jth period on the ith day (mW)
	A_k	Tasks executed on NVP_k, $k \in [1, N_k]$
	C_h	Capacity of the hth super capacitor (F), $h \in [1, H]$
Variable	$x_{i,j,m}(n)$	Scheduling results for task τ_n of the mth time slot in the jth period on the ith day
	$C_{h,i}$	Selected super capacitor size on the ith day (F)
	$V^{sc}_{i,j,m}(C_{h,i})$	Voltage of the super capacitor $C_{h,i}$ at the beginning of the mth time slot in the jth period on the ith day (V)
	$S'_{i,j,m}(n)$	Remaining execution time of τ_n at the beginning of the mth time slot in the jth period on the ith day (s)

3.1 Parameters of tasks and the system

Table 1 presents the parameters and variables of the system model. The parameters contain three parts: time, task and system.

In the applications of wireless sensor network (WSN), a set of real-time periodic tasks will be executed on the dual-channel solar-powered sensor node.

There are five time related parameters for long term scheduling. N_d is the number of days for scheduling. ΔT is the period of tasks and there are N_p periods on each day. A period can be further divided into N_s time slots, where each time slot is Δt. Considering intra-task scheduling, we assume that tasks can be preempted at the beginning of every time slot. In addition, tasks executed in one period are independent of those in others.

We use a directed acyclic graph $G(V, W)$ to describe the task parameters, where V is the task set and W is the edge set. In V, there are N tasks (denoted as τ_1, τ_2, $\cdots$, τ_N), which are executed by N_k NVPs. Each task (τ_n) has three parameters: the deadline (D_n), the total execution time (S_n) and the average execution power (P_n^τ) in each period. In W, $W_{n,l}$ denotes the task dependence from τ_n to τ_l. $W_{n,l} = 1$, if τ_l depends on the results of τ_n; otherwise, $W_{n,l} = 0$.

The system contains three parameters. $P^s_{i,j,m}$ denotes the average solar power of the mth time slot in the jth period on the ith day. A_k is a task set including the tasks executed on NVP_k. Note that a task can only be executed on a certain NVP while each NVP executes only one task at the same time. C_h is the capacity of the hth super capacitor and the total number of the distributed super capacitors on the sensor node is H.

3.2 Scheduling variables

The 0-1 variable $x_{i,j,m}(n)$ denotes the scheduling results for task τ_n of the mth time slot in the jth period on the ith day. $x_{i,j,m}(n) = 1$, if τ_n is executed; $x_{i,j,m}(n) = 0$, otherwise. $C_{h,i}$ is the selected super capacitor size used on the ith day.

Based on $x_{i,j,m}(n)$ and $C_{h,i}$, we define two intermediate variables: $V^{sc}_{i,j,m}(C_{h,i})$ and $S'_{i,j,m}(n)$. $V^{sc}_{i,j,m}(C_{h,i})$ is the voltage of the super capacitor $C_{h,i}$ at the beginning of the mth time slot in the jth period on the ith day and we have,

$$\begin{aligned}\tfrac{1}{2}\cdot C_{h,i}\cdot V^{sc\ 2}_{i,j,m+1}(C_{h,i}) = \tfrac{1}{2}\cdot C_{h,i}\cdot V^{sc\ 2}_{i,j,m}(C_{h,i})\\ -P_{leak}(V^{sc}_{i,j,m}(C_{h,i}))\cdot\Delta t\\ +\Delta E_{i,j,m}\cdot\eta(V^{sc}_{i,j,m}(C_{h,i}))\end{aligned} \tag{1}$$

where $P_{leak}()$ is the leakage function of the super capacitor. The function is obtained from data fitting with tested results of several capacitors. $\Delta E_{i,j,m}$ is the migrated energy of the mth time slot in the jth period on the ith day. $\eta()$ is the efficiency function of the super capacitor. $\Delta E_{i,j,m}$ and $\eta()$ are calculated as follows,

$$\Delta E_{i,j,m} = [P^s_{i,j,m} - \sum_{n=1}^{N} x_{i,j,m}(n)\cdot P^\tau_n]\cdot\Delta t \tag{2}$$

$$\eta(V^{sc}_{i,j,m}(C_{h,i})) = \begin{cases}\eta_{chr}(V^{sc}_{i,j,m}(C_{h,i}))\cdot\eta_{cycle}(C_{h,i}),\\ \text{if } \Delta E_{i,j,m} > 0 \& V^{sc}_{i,j,m}(C_{h,i}) < V_H(C_{h,i})\\ 1/[\eta_{dis}(V^{sc}_{i,j,m}(C_{h,i}))\cdot\eta_{cycle}(C_{h,i})],\\ \text{if } \Delta E_{i,j,m} < 0 \& V^{sc}_{i,j,m}(C_{h,i}) > V_L(C_{h,i})\\ 0, \text{otherwise}\end{cases} \tag{3}$$

$\eta_{chr}()$ is the efficiency function of the input regulator while $\eta_{dis}()$ is the efficiency function of the output regulator. The two functions are obtained from data fitting with the tested results in Figure 5. $\eta_{cycle}()$ is the average cycle efficiency of the super capacitor [12]. V_H and V_L are the full-charged and cut-off voltages of all the super capacitors, respectively. In addition, $\eta(V^{sc}_{i,j,m}(C_{h,i})) = 0$, if there is no energy migration or the voltage of the super capacitor is out of range.

$S'_{i,j,m}(n)$ is the remaining execution time of τ_n at the beginning of the mth time slot in the jth period on the ith day, which describes τ_n's current status. It is calculated as follows,

$$S'_{i,j,m}(n) = S_n - \sum_{l=1}^{m-1} x_{i,j,l}(n)\cdot\Delta t \tag{4}$$

That is, $S'_{i,j,m}(n) = S_n$, if τ_n has never been executed; $S'_{i,j,m}(n) = 0$, if τ_n is completed. We define a step function $\theta()$ to denote whether τ_n misses its deadline or not. The function is presented as follows,

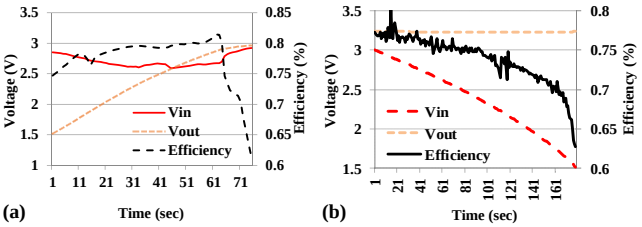

Figure 5: Tested efficiencies of input and output regulators

$$\theta(S'_{i,j,D_n}(n)) = \begin{cases}1 & \text{if } S'_{i,j,D_n}(n) > 0\\ 0 & \text{otherwise}\end{cases} \tag{5}$$

If $S'_{i,j,D_n}(n) > 0$, τ_n misses its deadline; otherwise, τ_n meets its deadline. The nearest beginning time of the next slot following D_n is used to calculate $S'_{i,j,D_n}(n)$, if D_n is not the beginning time of a time slot.

3.3 Problem formulation

The scheduling problem is described as an integer nonlinear programming (INLP) formulation. Our goal is to find the optimal scheduling results $\{x_{i,j,m}(n)\}$ and the optimal super capacitors $\{C_{h,i}\}$ that minimize the long term DMR.

$$\textit{objective:}\quad \min \frac{\sum_{i=1}^{N_d}\sum_{j=1}^{N_p}\sum_{n=1}^{N}\theta(S'_{i,j,D_n})}{N_d\cdot N_p\cdot N} \tag{6}$$

subject to:

$$S'_{i,j,m}(l) = S_l, \text{if } \sum_{n=1}^{N} W_{n,l}\cdot S'_{i,j,m}(n) > 0, \tag{7}$$

$$\sum_{m=1}^{N_s} x_{i,j,m}(n)\cdot\Delta t \le S_n \tag{8}$$

$$\sum_{\forall\tau_n\in A_k} x_{i,j,m}(n) \le 1, \forall k \in [1, N_k] \tag{9}$$

In the formulation, the constraint (7) means that τ_n starts only if all its depending tasks are completed. The constraint (8) means that the total execution time of τ_n cannot be violated. The constraint (9) means that an NVP can only run one task at the same time. However, the complexity of the formulation is $O(2^{N\cdot N_s\cdot N_p\cdot N_d}\cdot H^{N_d})$, which is equal to all the possible combinations of scheduling results and super capacitor selections. The formulation cannot be solved by traditional solvers (e.g. LINGO). Thus, we present some methods to simplify the formulation in Section 4.2.

4. OFFLINE OPTIMIZATION

This section first gives the method for super capacitor sizing and then simplifies the formulation (in Section 3.3) to get the optimal samples for offline ANN training.

4.1 Super capacitor sizing

Based on the motivation of super capacitor sizing in Section 2.1, we need to decide the capacities of H distributed super capacitors (C_h) at design time.

The procedure of super capacitor sizing contains three steps. First, we get the different energy migration patterns. As the probability of energy migration between days is quite small, we focus on the energy migration in a single day. Thus, we calculate the migrated energy ($\Delta E_{i,j,m}$) on each day with the corresponding solar power (see Equation (2)). The scheduling results for all the tasks ($x_{i,j,m}(n)$) are obtained based on the as soon as possible (ASAP) rule.

Second, we find the optimal capacity (C_i^{opt}) with the smallest energy loss during migration (including voltage converting, capacitor storage cycles and leakages) on the ith day.

$$\begin{aligned}\min\ \sum_{j=1}^{N_p}\sum_{m=1}^{N_s}[\Delta E_{i,j,m}\cdot(1-\eta(V^{sc}_{i,j,m}(C_i^{opt})))\\ +P_{leak}(V^{sc}_{i,j,m}(C_i^{opt}))\cdot\Delta t]\end{aligned} \tag{10}$$

The voltage at the beginning of the next time slot ($V^{sc}_{i,j,m+1}(C^{opt}_i)$) can be obtained with the current voltage ($V^{sc}_{i,j,m}(C^{opt}_i)$) as follows,

$$V^{sc}_{i,j,m+1} = [2 \cdot \Delta E_{i,j,m} \cdot \eta(V^{sc}_{i,j,m}(C^{opt}_i))/C^{opt}_i - 2 \cdot P_{leak}(V^{sc}_{i,j,m}(C^{opt}_i)) \cdot \Delta t/C^{opt}_i + V^{sc\ 2}_{i,j,m}]^{\frac{1}{2}} \quad (11)$$

Giving the initial voltage $V^{sc}_{i,1,1}(C^{opt}_i)$, we can get the voltage at the beginning of each time slot in each period recursively. In this way, the optimal capacity (C^{opt}_i) of the super capacitor on the ith day is obtained.

Finally, as the number of $\{C^{opt}_i\}$ (N_d) is usually larger than that of the distributed super capacitors (H), we cluster $\{C^{opt}_i\}$ into H sets based on the corresponding solar power. We use the average value of $\{C^{opt}_i\}$ in the hth set ($h \in [1, H]$) as the capacity of the hth super capacitor (C_h).

4.2 Optimization of offline long term DMR

As the original formulation (in Section 3.3) has prohibitive complexity, we simplify it by defining a new kind of variables $\{DMR_{i,j}\}$ to replace the original scheduling variables ($\{x_{i,j,m}(n)\}$). $DMR_{i,j}$ is the DMR of the jth period on the ith day. Thus, our goal is to find the optimal DMR in each period ($\{DMR_{i,j}\}$) and the optimal super capacitor on each day ($\{C_{h,i}\}$) that minimize the long term DMR. Thus, the goal of the simplified formulation is presented as follows,

$$\min [\sum_{i=1}^{N_d} \sum_{j=1}^{N_p} DMR_{i,j}]/(N_d \cdot N_p) \quad (12)$$

The variables ($DMR_{i,j}$ and $C_{h,i}$) correspond to a lookup table (LUT) as follows,

$$\{E^c_{i,j}, \{te_{i,j}(n)\}, \alpha_{i,j}\} = \mathrm{LUT}(DMR_{i,j}, \{P^s_{i,j,m}\}, C_{h,i}, V^{sc}_{i,j,1}(C_{h,i})) \quad (13)$$

In the LUT, the inputs have four parameters: the DMR ($DMR_{i,j}$), the solar power ($\{P^s_{i,j,m}\}, m \in [1, N_s]$), the super capacitor ($C_{h,i}$) and its initial voltage ($V^{sc}_{i,j,1}(C_h)$) in a period. The outputs contain three parameters: the minimum consumed energy of the super capacitor ($E^c_{i,j}$), the executed tasks ($\{te_{i,j}(n)\}$) and the index for scheduling pattern selection ($\alpha_{i,j}$) in a period. $E^c_{i,j}$ has a constraint as follows,

$$E^c_{i,j} \geq \frac{1}{2} \cdot C_{h,i} \cdot (V^{sc}_{i,j,1}{}^2(C_{h,i}) - V_L^2) \quad (14)$$

It means that the energy consumed by the super capacitor is no more than its total usable energy in a period. Furthermore, as the LUT has a limited number of items, we use the closest input in the LUT to approximate the real input, if the values of some parameters in the real input (e.g., the solar power and the voltage of the super capacitor) do not exist in the LUT.

By solving the optimization problem, including Equation (12) – (14), we can get the optimal long term DMR. The complexity of the formulation is $O((N+1)^{N_p \cdot N_d} \cdot H^{N_d})$, where $N+1$ and H are the numbers of values for $DMR_{i,j}$ and $C_{h,i}$, respectively.

In addition, the outputs in the LUT are generated by optimizing the scheduling variables ($\{x_{i,j,m}(n)\}$) based on the corresponding inputs. The optimization goal is to minimize the consumed energy of the super capacitor ($E^c_{i,j}$) as follows,

$$\min E^c_{i,j} = \frac{1}{2} \cdot C_{h,i} \cdot [V^{sc}_{i,j,1}{}^2(C_{h,i}) - V^{sc\ 2}_{i,j+1,1}(C_{h,i})] \quad (15)$$

And a DMR constraint is presented as follows,

$$\sum_{n=1}^{N} \theta(S'_{i,j,D_n}(n))/N = DMR_{i,j} \quad (16)$$

By solving the optimization problem, including Equation (7) – (9), (15) and (16), we can get the minimum consumed energy ($E^c_{i,j}$) and the optimal scheduling results ($\{x_{i,j,m}(n)\}$) in the period. The complexity of the formulation is $O(2^{N \cdot N_s})$.

Thus, the executed tasks ($\{te_{i,j}(n)\}$) can be calculated as follows,

$$te_{i,j}(n) = \begin{cases} 1, \text{if } \sum_{m=1}^{N_s} x_{i,j,m}(n) > 0 \\ 0, \text{otherwise} \end{cases} \quad (17)$$

$te_{i,j}(n) = 1$, if τ_i is executed in the period; otherwise, $te_{i,j}(n) = 0$. The index for scheduling pattern selection ($\alpha_{i,j}$) is calculated as follows,

$$\alpha_{i,j} = (\sum_{n=1}^{N} te_{i,j}(n) \cdot S_n \cdot P^{\tau}_n)/(\sum_{m=1}^{N_s} P^s_{i,j,m} \cdot \Delta t) \quad (18)$$

which is the ratio of the load consumption to the solar power supply. $\alpha_{i,j}$ is used for online scheduling (in Section 5.2).

The total complexity of the simplified optimization is $O(2^{N \cdot N_s} \cdot M + (N+1)^{N_p \cdot N_d} \cdot H^{N_d})$, where M is the number of items in the LUT. We then use the optimal variables and the corresponding parameters in the LUT as the samples for offline ANN training. After that, the weights of the ANN are achieved. In addition, the architecture of the ANN is presented in Section 5.1.

5. ONLINE SCHEDULING

This section first presents the online ANN-based long term deadline-aware analysis for each period. An online selection method is then given to utilize the ANN's outputs for the intra / inter-task scheduling in each time slot of the period.

5.1 Online ANN-based long term deadline-aware analysis

To realize the online long term deadline-aware scheduling, we first need to obtain the optimal capacitor, the executed tasks, the index for scheduling pattern selection based on the historical solar power, the voltages of all super capacitors and the current accumulated DMR at the beginning of each period. To capture the relationship among them effectively, we use a deep belief network (DBN), a deep learning ANN model.

The architecture of the DBN is shown in Figure 6. The inputs are the solar power of the last period ($P^s_{i,j-1,m}, m \in [1, N_s]$), the initial voltages of all super capacitors ($V^{sc}_{i,j,1}(C_h), h \in [1, H]$) and the current accumulated DMR ($DMR^{acc}_{i,j-1}$) at the beginning of the current period. $DMR^{acc}_{i,j-1}$ is calculated as follows,

$$DMR^{acc}_{i,j} = (\sum_{p=1}^{i} \sum_{q=1}^{j} DMR_{p,q})/[(i-1) \cdot N_d + j] \quad (19)$$

The outputs are the optimized capacitor of the day ($C_{h,i}$), the index for scheduling pattern selection ($\alpha_{i,j}$) and the tasks to be executed ($\{te_{i,j}(n)\}$) in this period. The DBN contains three parts: the inputs, the hidden layers and the visible layers for outputs. The hidden layers extract the features of the inputs by unsupervised learning on two kinds of networks: restricted Boltzmann machine (RBM) and sigmoid belief network. The visible layers calculate the outputs by a back propagation network (BPN).

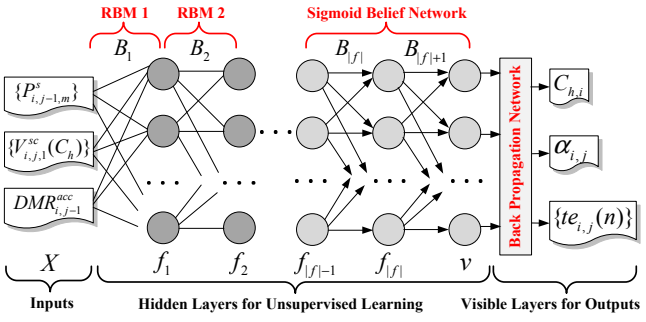

Figure 6: Architecture of DBN

We get the real-time optimized scheduling parameters for each period by online DBN calculation. First, a joint probability distribution function ($P(v, f_{|f|}..., f_1, X)$) is calculated based on the input vector (X) as follows,

$$P(v, f_{|f|}..., f_1, X) = P(v|f_{|f|}) \cdots P(f_1, X) \quad (20)$$

where $\{f_1, .., f_{|f|}\}$ denotes the set of $|h|$ hidden units and v is the visible unit. The conditional probability functions in Equation 20 are independent of each other and they are calculated as follows,

$$P(v|f_{|f|}) = \prod_p P(v_p|f_{|f|})$$
$$P(v_p|f_{|f|}) = (1 + \exp(-\sum_q B_{|f|+1,p,q} \cdot h_q^1))^{-1} \quad (21)$$
$$P(f_1, X) = (1 + \exp((f_1)^T \cdot B_1 \cdot X))^{-1}$$

where $\{B_1, ..., B_{|f|+1}\}$ are the weights of the hidden layers. The outputs are then obtained by calculating the BP network [9] based on the visible unit (v). All the weights of the DBN are offline trained layer by layer based on the samples obtained in Section 4.2.

5.2 Online selection method for the ANN's outputs

After the online ANN calculation, the optimized super capacitor ($C_{h,i}$) and the index for scheduling pattern selection ($\alpha_{i,j}$) in each period are achieved. As the predicted solar power may be inaccurate at the beginning of each day, the optimized super capacitor ($C_{h,i}$) may be changing among different periods. However, it is inefficient to change from a super capacitor with large energy to those with little energy, as the energy migration efficiency is quite low. Thus, we introduce a threshold energy (E_{th}) to decide whether to change the super capacitor (C_{use}) or not. If the energy stored in the super capacitor C_{use} is smaller than E_{th}, it will be changed to the optimal $C_{h,i}$ obtained from the ANN; otherwise, it will not be changed. The judgment formula is listed as below,

$$C_{use} = \begin{cases} C_{h,i}, \text{if } \frac{1}{2} \cdot C_{use} \cdot (V_{i,j,1}^{sc\ 2}(C_{use}) - V_L^2) < E_{th} \\ C_{use}, \text{otherwise} \end{cases} \quad (22)$$

Moreover, we notice that if the index for scheduling pattern selection ($\alpha_{i,j}$) is too large or too small (e.g. at night), the intra-task scheduling is unnecessary. In this situation, we can just use the simple inter-task scheduling to save energy and time. Therefore, we introduce a threshold δ for scheduling pattern selection. If $|1 - \alpha| > \delta$, the inter-task scheduling is used; otherwise, the intra-task scheduling is performed for better DMR.

6. EXPERIMENTAL EVALUATION

In this section, the experimental setup and energy migration validation are first presented. The proposed algorithm is then compared with the traditional best local DMR schedulers, as well as a static optimal scheduler as an upper bound. Furthermore, the solar prediction length and the number of super capacitors in the algorithm are analyzed. Finally, we present the overhead of the algorithm.

6.1 Experimental setup

In the experiments, six benchmarks are evaluated for wireless sensor applications. Three of them are random benchmarks, where the task number ranges from 4 to 8, the edge number is from 0 to 2 and the NVP number is from 2 to 6. The real benchmarks consist of wild animal monitoring (WAM)[1], electrocardiogram applications (ECG)[2] and structure health monitoring (SHM)[3]. The tasks in these benchmarks are implemented by a C2RTL tool based on the C codes. We use Modelsim and DC compiler to acquire the execution time and power of these tasks under the SMIC 130nm technology.

The system parameters are extracted based on the dual-channel solar-powered sensor node [11], which contains a direct solar supply channel and an energy migration channel with distributed super capacitors. The area and tested average converting efficiency of the solar panel are $3.5{\times}4.5cm^2$ and 6%. A real solar database [15] is used. Solar power of four individual days (see Figure 7) representing different patterns in a whole year are selected for daily test and those of two-month are used for monthly test.

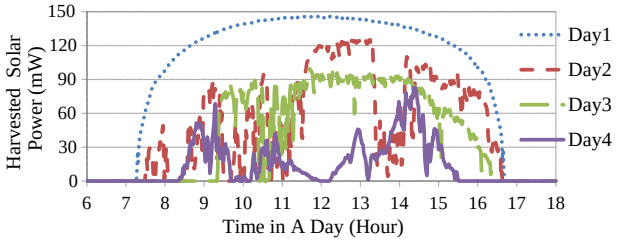

Figure 7: Solar power of four individual days

6.2 Energy migration validation

We validate our model by energy migration test. Table 2 presents the migration efficiencies calculated by our model and the measurements on the proposed sensor node with different super capacitors (F), migration quantities (J) and distances (min). The average error of our model is 5.38%, which is reasonable for task scheduling optimization. In addition, the optimal capacity with the highest efficiency varies (from $1F$ to $10F$) in quantity and distance of energy migration (from $7J$, $60min$ to $30J$, $400min$). It is because the energy loss of charging, discharging and leakage of different capacitors changes with energy migration patterns. The largest difference of efficiency among these capacitors is 30.5%, which proves the necessity of sizing for the distributed super capacitors.

Table 2: Energy migration efficiencies with different capacitors

Capacity	$7J$, $60min$			$30J$, $400min$		
	Model	Test	Error	Model	Test	Error
$1F$	36.8%	40.5%	9.13%	8.58%	9.46%	9.30%
$10F$	27.8%	27.3%	1.83%	40.7%	40.0%	1.75%
$50F$	25.9%	25.0%	3.60%	27.3%	26.7%	2.25%
$100F$	25.0%	23.1%	8.23%	20.1%	18.8%	6.91%

6.3 Performance comparison

The proposed algorithm (Proposed) is compared with an up-to-date WCMA-based LSA (Inter-task) [3] and an intra-task scheduler [9] (Intra-task). A static optimal scheduler (in Section 4.2) is provided as an upper bound based on the given solar power (Optimal). Figure 8 shows the DMRs of all the algorithms for six benchmarks in four individual days. Compared with [3], the proposed method reduces DMR by up to 27.8% and its average DMR has a difference of 3.69% with the optimal scheduler. Furthermore, the proposed method has better DMR when the solar energy decreases (from Day1 to Day4).

We also study the relationship between DMR and energy utilization for the WAM case in two months. Figure 9 (a) shows that the DMRs obtained from the proposed algorithm are closer to the optimal results. However, the energy utilizations of the proposed one are lower than those of [3] and [9]. The average differences are 5.53% and 10.6% (see Figure 9 (b)), respectively. It is because more energy is migrated in the proposed method, which leads to more energy loss of super capacitors for long term DMR. ***Thus, it implies that traditional optimizing objective to maximize energy utilization does not necessarily lead to better DMR.***

6.4 Scheduling analysis

For long term scheduling with the proposed algorithm, the DMR is affected by several factors, such as the solar prediction length, the number of super capacitors, the numbers of layers and neurons in the ANN as well as the thresholds in the selection method. Among them, the solar prediction length and the number of super capacitors are the most important ones.

[1] The WAM case contains eight tasks: periodic locating, heart rate sampling, voice recordation, audio process, emergency response, audio compression, local storage and data transmission.
[2] The six tasks are in ECG and they are low pass filter, high pass filter 1/2, QRS wave detection, FFT and AES encoder.
[3] The five tasks are temperature sensing, acceleration sensing, FFT, data receiving and transmitting.

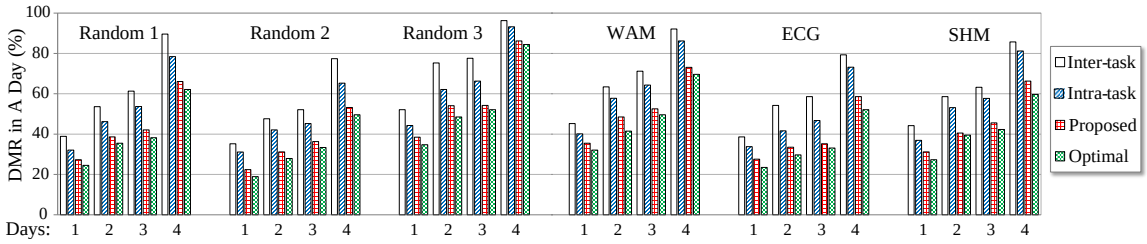

Figure 8: DMR in four individual days with six benchamrks

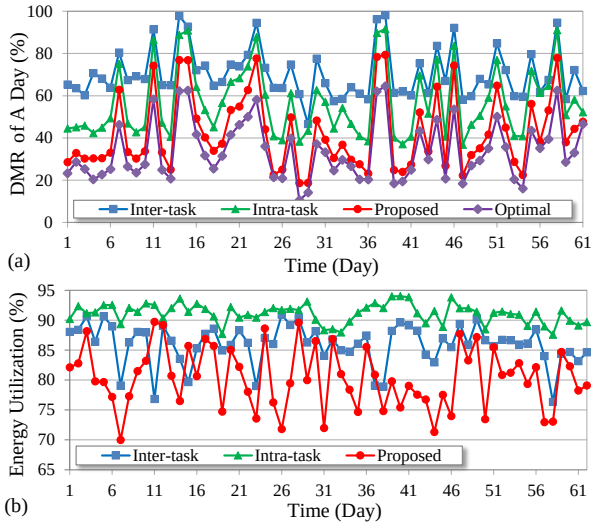

Figure 9: DMR and energy utilization in two months

Figure 10 (a) presents the DMRs and complexities under different solar prediction lengths for the random case 1 in a month. As we can see, better long term DMR can be achieved if the prediction length becomes larger and the optimal DMR is 68.9% with a prediction length of 48 hours. ***However, the DMR becomes even worse (70.2%) when the prediction length is larger (96 hours) than the certain threshold (48 hours in this case).*** Based on the analysis of the solar power, we find that it is because a long prediction for solar power is inaccurate, which degrades the DMR. Though this inaccurate prediction makes the DMR worse, the degradation speed is quite slow (from 68.9% to 70.2%). This phenomenon can be explained by the fact that the probability of energy migration among several days is quite small, since energy in the super capacitor is used up at night in most cases. Finally, since the complexity for a long prediction length increases exponentially, we should select a suitable prediction length based on the tradeoff of DMR and complexity.

We then analyze super capacitor sizing under different numbers of super capacitors for the random case 1 in Day 2. As the number of distributed super capacitors increases (from 1 to 8) in Figure 10 (b), the efficiency of energy migration turns higher (from 67.5% to 87.1%) and the DMR becomes lower (from 46.8% to 33.7%). The DMR stays the same with five or more super capacitors, because small improvements on energy migration cannot reduce DMR any more.

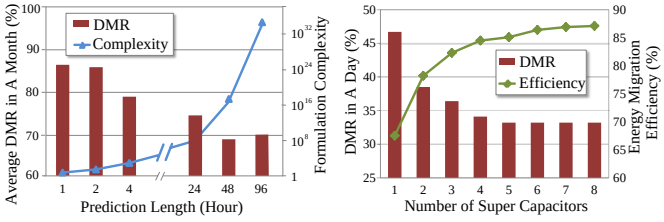

Figure 10: Prediction length and number of super capacitors

6.5 Algorithm overhead

Finally, we analyze the overhead of the algorithm. We run the algorithm on the proposed sensor node at $93.5kHz$. The execution delay is obtained from an oscilloscope and the power consumption is sampled by a data acquisition board (DAQ) on the Labview. The time and power of the coarse-grained / fine-grained procedure per execution are $14.6s$ / $3.47s$ and $3.0mW$ / $2.94mW$. Compared with the normal workloads on the node, the algorithm brings less than 3% of the total energy consumption.

7. CONCLUSIONS

In this paper, we propose a long term deadline-aware scheduling algorithm with energy migration strategies for the distributed super capacitors. It contains offline and online parts. The offline part determines the optimal capacitor sizes and DMR training samples for an ANN. The online part adopts the ANN to determine the real-time optimal capacitor size, scheduling pattern and task queue, followed by an intra / inter-task scheduling algorithm for better DMR. Experimental results show that the proposed algorithm reduces DMR by 27.8% and brings less than 3% of the total energy consumption.

8. REFERENCES

[1] C. Moser, L. Thiele, et al. Adaptive power management in energy harvesting systems. In *DATE*, pages 773–778, 2007.

[2] C. Moser, J. Chen, et al. Reward maximization for embedded systems with renewable energies. In *RTCSA*, pages 247–256, 2008.

[3] J. Piorno, C. Bergonzini, et al. Hollows: A power-aware task scheduler for energy harvesting sensor nodes. *Journal of Intelligent Material Systems and Structures*, 21(12):1317–1335, 2010.

[4] T. Zhu, A. Mohaisen, et al. Deos: Dynamic energy-oriented scheduling for sustainable wireless sensor networks. In *INFOCOM*, pages 2363–2371, 2012.

[5] S. Liu, J. Lu, et al. Load-matching adaptive task scheduling for energy efficiency in energy harvesting real-time embedded systems. In *ISLPED*, pages 325–330, 2010.

[6] S. Liu, J. Lu, et al. Harvesting-aware power management for real-time systems with renewable energy. *IEEE Transactions on Very Large Scale Integration Systems*, 20(8):1473–1486, 2012.

[7] Y. Wang, R. Chen, et al. Solartune: Real-time scheduling with load tuning for solar energy powered multicore systems. In *RTCSA*, pages 101–110, 2013.

[8] X. Lin, Y. Wang, et al. A framework of concurrent task scheduling and dynamic voltage and frequency scaling in real-time embedded systems with energy harvesting. In *ISLPED*, pages 70–75, 2013.

[9] D. Zhang, S. Li, et al. Intra-task scheduling for storage-less and converter-less solar-powered nonvolatile sensor nodes. In *ICCD*, pages 348–354, 2014.

[10] C. Wang, N. Chang, et al. Storage-less and converter-less maximum power point tracking of photovoltaic cells for a nonvolatile microprocessor. In *ASPDAC*, pages 379–384, 2014.

[11] X. Sheng, C. Wang, et al. A high-efficiency dual-channel photovoltaic power system for nonvolatile sensor nodes. In *NVMSA*, pages 1–2, 2014.

[12] D. Brunelli, C. Moser, et al. Design of a solar-harvesting circuit for battery-less embedded systems. *IEEE Transactions on Circuits and Systems I*, 56(11):2519–2528, 2009.

[13] Y. Wang, Y. Liu, et al. A 3us wake-up time nonvolatile processor based on ferroelectric flip-flops. In *ESSCIRC*, pages 149–152, 2012.

[14] Y. Wang, Y. Liu, et al. Pacc: A parallel compare and compress codec for area reduction in nonvolatile processors. *IEEE Transactions on Very Large Scale Integration Systems*, 22(7):1491–1505, 2014.

[15] Measurement and Instrumentation Data Center (MIDC), http://www.nrel.gov/midc/.